Journal of Applied Mathematics and Physics, 2013, 1, 5-15
Published Online December 2013 (http://www.scirp.org/journal/jamp)
http://dx.doi.org/10.4236/jamp.2013.17002

Discrete Singular Convolution Method for Numerical Solutions of Fifth Order Korteweg-De Vries Equations

Edson Pindza, Eben Maré
Department of Mathematics and Applied Mathematics,
University of Pretoria, Pretoria, South Africa
Email: eben.mare@up.ac.za

Received October 7, 2013; revised November 7, 2013; accepted November 15, 2013

ABSTRACT

A new computational method for solving the fifth order Korteweg-de Vries (fKdV) equation is proposed. The nonlinear partial differential equation is discretized in space using the discrete singular convolution (DSC) scheme and an exponential time integration scheme combined with the best rational approximations based on the Carathéodory-Fejér procedure for time discretization. We check several numerical results of our approach against available analytical solutions. In addition, we computed the conservation laws of the fKdV equation. We find that the DSC approach is a very accurate, efficient and reliable method for solving nonlinear partial differential equations.

Keywords: Fifth Order Korteweg-De Vries Equations; Discrete Singular Convolution; Exponential Time Discretization Method; Soliton Solutions; Conservation Laws

1. Introduction

The study of travelling wave solutions of nonlinear partial differential equations (PDEs) is the major subject in many fields of physical and nonlinear sciences. Concepts like solitons, peakons, kinks, breathers, cusps and compactons have entered into various branches of natural sciences such as chemistry, biology, mathematics, communication and particularly in almost all branches of physics like the fluid dynamics, plasma physics, field theory, nonlinear optics and condensed matter physics. Among these nonlinear PDEs there exists an important class of the fifth order Korteweg-de Vries equations

$$u_t + \alpha u u_{3x} + \beta u_x u_{2x} + \lambda u^2 u_x + u_{5x} = 0, \tag{1}$$

where $u_{kx} = \partial^k u / \partial x^k$ α, β and λ are real numbers. This class includes the well-known Lax [1], Sawada-Kotera (SK) [2], Kaup-Kupershmidt (KK) [3] and Ito [4] equations. The knowledge of close form solutions of nonlinear PDEs facilitates the verification of numerical solvers, aids physicists to better understand the mechanism that governs the physic models, provides knowledge to the physical problem, provides possible applications and helps mathematicians in the stability analysis of solutions. While strange attractors and chaos theory give us a better understanding of the erratic and often unpredictable nature of natural phenomena, and soliton theory helps explain natural phenomena that are surprisingly predictable and regular even under conditions that would normally destroy such properties. A soliton is a solitary wave which preserves its shape and velocity after nonlinearly interacting with other solitary waves or (arbitrary) localized disturbances.

In general, Equation (1) does not admit exact solutions, therefore one has to resort to numerical methods. Due to the fifth-order terms in these equations, it is very difficult to compute the solutions of these equations accurately and efficiently. Recently, Shen [5] proposed a new dual-Petrov-Galerkin method for the third and higher odd-order equations. His approach was proven to be very effective for the KdV type equations in bounded domains [5] and in semi-infinite intervals [6]. In [7], a numerical scheme based on the dual-Petrov-Galerkin method was proposed and implemented for the Kawahara and modified Kawahara equations.

In this paper, we propose a discrete singular convolution method to solve fifth order Korteweg-de Vries equations. Discrete singular convolution (DSC) methods belong to the family of local spectral (LS) methods. They were proposed by Wei [8] as a potential approach for numerical realization of the Hilbert transform, Abel transform, Random transform and Delta transform. The DSC algorithm has been essential to many practical applications, such as nonlinear equations [9], structural analysis [10,11], compressible and incompressible fluid flows [12,13], electromagnetic wave propagation, scattering [14, 15] and image analysis [16].

Recently, Pindza and Maré [17] utilized a combined fourth order exponential time differencing of Adams type and the DSC method to solve the generalized Korteweg-de Vries. Their approach revealed exponential convergence. The advantage of the DSC methods is that they exhibit exponential convergence of spectral methods [18] while having the flexibility of local methods for complex boundary conditions [10,19].

The discretization of the generalized Korteweg-de Vries equations in space with the DSC method yields a system of ordinary differential equations (ODE) that needs to be solved by time integration methods. We use the fourth order exponential time differencing Runge Kutta (ETDRK4) [20] for the solution of the resulting semi-discrete equations. The matrix exponential required by the scheme is efficiently computed using best rational approximations based on the Carathéodory-Fejér (CF) procedure [21].

The layout of this paper is as follows. We describe the formulation of the DSC method in Section 2. In Section 3, we discuss the exponential time integration methods for solving the semi-discrete system resulting from the spatial discretization of the nonlinear PDEs. Numerical results illustrating the merits of the new scheme are given in Section 4 and we present our conclusions in Section 5.

2. Discrete Singular Convolution Methods

Discrete singular convolution (DSC) methods are relatively new numerical techniques in the field of nonlinear equations. They are defined as follow. Consider a distribution, T and $\eta(t)$ an element of the space of test functions. A singular convolution can be defined by

$$F(t)=\int_{-\infty}^{\infty}T(t-x)\eta(x)\,\mathrm{d}x\mathrm{e}^{x} \tag{2}$$

where $T(t-x)$ is a singular kernel. For many science and engineering problems, an appropriate choice of T has to be done. For instance, in the field of interpolation of surfaces and curves the singular kernel of delta type $T(x)=\delta(t)$ is very important. For numerical solutions of partial differential equations, the kernel $T(x)=\delta^{(n)}(t), n=0,1,\cdots,$ is essential, where the subscript n denotes the n-th order derivative of the distribution with respect to parameter x. While using the DSC method, numerical approximations of a function and its derivatives can be treated as convolutions with some kernels. According to the DSC method, the n-th derivative of a function $f(x)$ can be approximated as [22]

$$f_{M,\sigma}^{(n)}(x)=\sum_{k=-M}^{M}\delta_{h,\sigma}^{(n)}(x-x_k)f(x_k), n=0,1,\cdots, \tag{3}$$

where h is the grid spacing, x_k is the set of discrete grid points which are centered around x, and $2M+1$ is the effective kernel, or computational bandwidth; and is usually smaller than the whole computational domain.

In the present paper, we focus our attention on the regularized Shannon kernel (RSK)

$$\delta_{h,\sigma}(x-x_k)=\frac{\sin\left[(\pi/h)(x-x_k)\right]}{(\pi/h)(x-x_k)}\mathrm{e}^{\left[\frac{-(x-x_k)^2}{2\sigma^2}\right]}, \sigma>0, \tag{4}$$

to provide discrete approximations to the singular convolution kernels of the delta type (3). The required derivatives of the DSC kernels can be easily obtained using ([12])

$$\delta_{i,j}^{(n)}=\delta_{i,j}^{(n)}(x_i-x_j)=\frac{\mathrm{d}^n}{\mathrm{d}x^n}\left[\delta_{h,\sigma}(x_i-x_j)\right]\Big|_{x=x_i} \tag{5}$$

The error estimation of the regularized Shannon kernel (RSK) delivers very small truncation errors when it uses the above convolution algorithm ([23])

Theorem 2.1 (Qian [23]). *Let* $f\in L^{\infty}(\mathbb{R})\cap L^{2}(\mathbb{R})\cap C^{n}(\mathbb{R})$ *be a function and band limited to* $B(B<\pi nh)$,

$n\in\mathbb{Z}^{+}, \sigma=rh>0, M\in\mathbb{N}\left(M\geq\frac{nr}{\sqrt{2}}\right)$. *Then*

$$f^{(n)}-f_{M,\sigma L^{\infty}(\mathbb{R})}^{(n)}\leq\beta\exp\left(\frac{-\alpha^2}{2r^2}\right), \tag{6}$$

where $\alpha=\min\left\{M,r^2(\pi-Bh)\right\}$ and

$$\beta=\frac{\mathrm{e}^{\pi}r(n+1)!}{h^n\pi\alpha}\left(\sqrt{2B}\|f\|_{L^2(\mathbb{R})}+2r\|f\|_{L^{\infty}(\mathbb{R})}\right)$$

Here N *is the number of grid points. The* L^{∞} *error given by* (6) *decays exponentially with respect to the increase of the DSC band width* M.

The proof of the above theorem is beyond the scope of this paper. We refer the reader to [23] for a detailed discussion on the Shannon's sampling theorem.

Using (4) and (5), the entries of the first, second, third and fifth differentiation matrices $D^{(1)}$, $D^{(2)}$, $D^{(3)}$ and $D^{(5)}$ are given explicitly by

$$\delta_{i,j}^{(1)}=\begin{cases}\dfrac{(-1)^{i-j}}{h(i-j)}\exp\left(\dfrac{-h^2(i-j)^2}{2\sigma^2}\right), & i\neq j\\ 0, & i=j\end{cases} \tag{7}$$

$$\delta_{i,j}^{(2)} = \begin{cases} 2(-1)^{i-j+1}\left(\dfrac{1}{h^2(i-j)^2}+\dfrac{1}{\sigma^2}\right)\times\exp\left(\dfrac{-h^2(i-j)^2}{2\sigma^2}\right), \\ \hfill i \neq j \\ -\dfrac{1}{3}\left(\dfrac{3}{\sigma^2}-\dfrac{\pi^2}{2\sigma^2}\right), \hfill i = j \end{cases} \tag{8}$$

$$\delta_{i,j}^{(3)} = \begin{cases} (-1)^{i-j}\left(\dfrac{\pi^2}{h^3(i-j)}+\dfrac{2}{h^3(i-j)^3}+\dfrac{3}{h\sigma^2(i-j)} \right. \\ \left. +\dfrac{3h(i-j)h-}{\sigma^4}\right)\times\exp\left(\dfrac{-h^2(i-j)^2}{2\sigma^2}\right), i \neq j \\ -\dfrac{1}{3}\left(\dfrac{3}{\sigma^2}-\dfrac{\pi^2}{2\sigma^2}\right), \hfill i = j \end{cases} \tag{9}$$

$$\delta_{i,j}^{(5)} = \begin{cases} (-1)^{i-j}\left[\dfrac{\pi^4}{i-j}+5\left(\dfrac{24}{(i-j)^5}+\dfrac{h^8(i-j)^3}{\sigma^3} \right.\right. \\ \left. -\dfrac{2h^6(i-j)}{\sigma^6}+\dfrac{3h^4}{\sigma^4(i-j)}+\dfrac{12h^2)h-}{(i-j)^3\sigma^2}\right) \\ \left. -\dfrac{10\pi^2\left(h^4(i-j)^4+h^2(i-j)^2\sigma^2+2\sigma^4\right)}{(i-j)^3\sigma^4}\right] \\ \times\exp\left(\dfrac{-h^2(i-j)^2}{2\sigma^2}\right), \hfill i \neq j \\ 0, \hfill i = j \end{cases} \tag{10}$$

Note that the differentiation matrix in (5) is in general banded. This gives rise to great advantage in large scale computations. Extension to higher dimensions can be realized by tensor products.

The choice of M, σ and h was suggested by Qian and Wei [23]. For instance, if the L^2 norm error is set to $10^{-\eta}\,(\eta > 0)$ the following relations must be satisfied

$$r(\pi - Bh) > \sqrt{4.6\eta} \quad \text{and} \quad \frac{M}{r} > \sqrt{4.6\eta} \tag{11}$$

where $r = \sigma/h$ and B is the frequency bound of the underlying function f.

To illustrate the procedure of discretization of PDEs by the DSC method, we consider the computation of fifth order KdV equations given by

$$u_t + \alpha u u_{3x} + \beta u_x u_{2x} + \lambda u^2 u_x + u_{5x} = 0, \tag{12}$$

where $u_{kx} = \partial^k u/\partial x^k$, α, β and λ are real numbers and $u \equiv u(x,t) \in C^\infty$.

This equation was previously considered in [24] where its properties were studied and its analytical soliton solutions were revealed. In the present paper we mainly focus on numerical solutions of Equation (12) via the use of DSC method.

The semi-discretized version, at the i th row, of the equation in consideration is obtained by substituting the relations (3) and (5) into (12), yielding

$$\begin{aligned} \frac{\partial u}{\partial t}(x_i,t) = & -\alpha u(x_i,t)\sum_{j=-M}^{M}\delta_{i,j}^{(3)}u(x_j,t) \\ & +\beta\sum_{j=-M}^{M}\delta_{i,j}^{(3)}u(x_j,t)\sum_{j=-M}^{M}\delta_{i,j}^{(3)}u(x_j,t) \\ & -\gamma u(x_i,t)^2\sum_{j=-M}^{M}\delta_{i,j}^{(3)}u(x_j,t) \\ & -\sum_{j=-M}^{M}\delta_{i,j}^{(3)}u(x_j,t) \end{aligned} \tag{13}$$

where $\delta_{i,j}^{(1)}$, $\delta_{i,j}^{(2)}$, $\delta_{i,j}^{(3)}$ and $\delta_{i,j}^{(5)}$ are the typical elements of matrices $D^{(1)}$, $D^{(2)}$, $D^{(3)}$ and $D^{(5)}$, respectively. Therefore, Equation (13) can be expressed in the following matrix form

$$\frac{\mathrm{d}u(t)}{\mathrm{d}t} = Lu(t) + N(t,u(t)) \tag{14}$$

where $L = D^{(5)}$ represents the linear part of the system and $N = -\alpha u\left(D^{(3)}u\right) - \beta\left(D^{(1)}u\right)\left(D^{(2)}u\right) - \gamma u^2\left(D^{(1)}u\right)$ represents the nonlinear part.

The main difficulty when dealing with systems of the type (14) is that the use of explicit time integrators is inefficient because the system typically suffers from instability due to the higher order derivative. This was emphasized by Pindza [25]. Consequently, the time step size must be significantly reduced in order to fulfill the drastic stability condition present in explicit time integrators. In this paper we use the fourth order exponential time differencing Runge-Kutta method.

3. Exponential Time Differencing

Exponential time differencing (ETD) schemes are known for a long time in computational electrodynamics; see [26] for a comprehensive review of ETD methods and their history. In this section, we describe the exponential time differencing fourth-order Runge-Kutta (ETD4RK) method which was proposed by Cox-Matthews [27].

The main idea of the ETD methods is to multiply both sides of a differential equation by some integrating factor, then we make a change of variable that allows us to solve the linear part exactly and, finally, we use a numerical method of our choice to solve the transformed nonlinear part.

3.1. Overview of the Method

In order to elaborate on this approach, let us consider the following semi-linear partial differential equation

$$u_t = Lu(t) + N(u,t) \tag{15}$$

where L and N are the linear and nonlinear operators, respectively. The semi-linear partial differential equation is discretized in space with the discrete singular convolution method. Therefore, we obtain a system of ordinary differential equations (ODEs)

$$\dot{u} = Lu(t) + N(u,t) \tag{16}$$

The exponential time differencing (ETD) methods can be obtained by integrating Equation (16) exactly between the time steps t_n and $t_{n+1} = t_n + h$ with respect to t, to obtain

$$u_{n+1} = \mathrm{e}^{Lh} u_n + \mathrm{e}^{Lh} \int_0^h \mathrm{e}^{-Lh} N\left(u\left(t_n + \tau\right), t_n + \tau\right) \mathrm{d}\tau \tag{17}$$

There exist various ETD methods for the evaluation of (17). The purpose of this work is not to give a complete classification of ETD methods. We focus specifically on the fourth order exponential time differencing Runge-Kutta (ETDRK4) given by

$$\begin{aligned}
a_n &= \mathrm{e}^{\frac{Lh}{2}} u_n + L^{-1}\left(\mathrm{e}^{\frac{Lh}{2}} - I\right) N\left(u_n, t_n\right), \\
b_n &= \mathrm{e}^{\frac{Lh}{2}} u_n + L^{-1}\left(\mathrm{e}^{\frac{Lh}{2}} - I\right) N\left(a_n, t_n + h/2\right), \\
c_n &= \mathrm{e}^{\frac{Lh}{2}} u_n + L^{-1}\left(\mathrm{e}^{\frac{Lh}{2}} - I\right)\left[2N\left(b_n, t_n + h/2\right) - N\left(u_n, t_n\right)\right], \\
u_{n+1} &= \mathrm{e}^{Lh} u_n + h^{-2} L^{-3}\left\{\left[-4I - hL + \mathrm{e}^{Lh}\left(4I - 3hL + (hL)^2\right)\right]\right. \\
&\quad N\left(u_n, t_n\right) + 2\left[2I + hL + \mathrm{e}^{Lh}\left(-2I + hL\right)\right] \\
&\quad \left(N\left(a_n, t_n + h/2\right) + N\left(b_n, t_n + h/2\right)\right) \\
&\quad + \left[-4I - 3hL - (hL)^2 + \mathrm{e}^{Lh}\left(4I - hL\right)\right] N\left(c_n, t_n + h\right)
\end{aligned} \tag{18}$$

The main computational challenge in the implementation of exponential time differencing (ETD) methods is the need for fast and stable evaluations of exponential and related φ-functions

$$\varphi_j(z) = \frac{1}{(j-1)!} \int_0^1 \mathrm{e}^{(1-\theta)z} \theta^{j-1} \mathrm{d}\theta, \ j \geq 0, \tag{19}$$

i.e., functions of the form $\left(\mathrm{e}^z - 1\right)/z$. The computation of these functions depends significantly on the structure and the range of eigenvalues of the linear operator and the dimensionality of the semi-discretized PDE. Unfortunately, for DSC methods the linear part have eigenvalues approaching zero, which leads to complications in the computation of the coefficients. Saad [28], and Hochbruck and Lubich [29] introduced Kyrlov methods to compute φ-functions. Kassam and Trefethen [20] used Cauchy integral representation on a circle for a stable computation of φ-functions. Our evaluation of exponential and related φ-matrix functions follows the idea of Schmelzer and Trefethen [30]. This method is based on computing optimal rational approximations to the matrix functions on the negative real axis using the Carathéodory-Fejér (CF) procedure [21], closely. The φ-functions (19) can be computed explicitly by a recursive formula

$$\begin{cases}
\varphi_0(z) = \mathrm{e}^z \\
\varphi_j(z) = \dfrac{\varphi_{j-1}(z) - \varphi_{j-1}(0)}{z}, \ j \geq 1
\end{cases} \tag{20}$$

Another way to compute the functions φ_j is to use the Taylor series representation. Therefore, for all complex numbers z, we have

$$\varphi_j(z) = \sum_{k=j}^{\infty} \frac{1}{k!} z^{k-j} \tag{21}$$

However, it is known that the computation of these functions in their explicit or Taylor series form suffers from computational inaccuracy for matrices whose eigenvalues are equal to or approaching zero. This is generally the case when the spatial discretization is based on spectral methods. In order to overcome the numerical difficulties encountered in the computation of (20) and (21), a different tactic for evaluating the function was proposed in [20]. The key idea is to approximate the functions (for matrices or scalars) by means of contour integrals in the complex plane

$$\varphi_j(z) = \frac{1}{2\pi i} \int_\Gamma \frac{\varphi_j(s)}{s - z} \mathrm{d}s = \frac{1}{M} \sum_{\ell=j}^{M} \varphi_j\left(z + \mathrm{e}^{i\theta_\ell}\right), \tag{22}$$

where $\theta_\ell = \dfrac{2\pi\ell}{M}$. If the contour Γ encloses the spectrum of the non-diagonal matrix L we have

$$\varphi_j(L) = \frac{1}{2\pi i} \int_\Gamma \varphi_j(s)(sI - L)^{-1} \mathrm{d}s. \tag{23}$$

If the size of the matrix L is large, it is more advantageous to compute the product of the functions $\varphi_j(z)$ and vectors b rather than to compute $\varphi_j(z)$ explicitly. We have

$$\begin{aligned}
\varphi_j(A)b &= \frac{1}{2\pi i} \int_\Gamma \varphi_j(s)(sI - L)^{-1} b \mathrm{d}s \\
&\approx \sum_{\ell=1}^{n} c_\ell \left(s_\ell I - L\right)^{-1} b,
\end{aligned} \tag{24}$$

where s_ℓ and c_ℓ are the poles and the residues, respectively. The sum in (24) is evaluated by solving at most n shifted linear systems. The poles and the residues are computed efficiently in standard precision by the Carathéodory-Fejér method [21,30].

3.2. Stability Analysis

In this section, we investigate the linear stability of the ETDRK4 method for the nonlinear autonomous system of ODEs,

$$\dot{u} = Lu + N(u), \tag{25}$$

linearized about a fixed point u_0 such that $Lu_0 + N(u_0) = 0$ We obtain

$$\dot{u} = Lu + \lambda u \tag{26}$$

where *u* is now the perturbation of u_0 and $\lambda = N'(u_0)$ is a diagonal or a block diagonal matrix containing the eigenvalues of N. If $\mathrm{Re}(L+\lambda) < 0$, then the fixed point u_0 is stable for all λ.

The stability region is four-dimensional, if both L and λ are complex. The two-dimensional stability region is obtained if both L and λ are purely imaginary or purely real, or if λ is complex and L is fixed and real.

In the paper, we follow the analysis employed in [27] and we only concentrate on the case where L and λ are real. We define $u_n = r^n(x,y)$, $x = \lambda y$ and $x = Lh$. Then, applying the ETDRK4 method (18) to the linearized problem (26) yields

$$r(x,y) = c_0 + c_1 x + c_2 x^2 + c_3 x^3 + c_4 x^4, \tag{27}$$

$$c_0 = \mathrm{e}^y$$

$$c_1 = -\frac{4}{y^3} + \frac{8\mathrm{e}^{y/2}}{y^3} - \frac{8\mathrm{e}^{3y/2}}{y^3} + \frac{4\mathrm{e}^{2y}}{y^3} - \frac{1}{y^2} + \frac{4\mathrm{e}^{y/2}}{y^2} - \frac{6\mathrm{e}^{y}}{y^2} + \frac{4\mathrm{e}^{3y/2}}{y^2} - \frac{\mathrm{e}^{2y}}{y^2}$$

$$c_2 = -\frac{8}{y^4} + \frac{16\mathrm{e}^{y/2}}{y^4} - \frac{16\mathrm{e}^{3y/2}}{y^4} + \frac{8\mathrm{e}^{2y}}{y^4} - \frac{5}{y^3} + \frac{12\mathrm{e}^{y/2}}{y^3} - \frac{10\mathrm{e}^{y}}{y^3} + \frac{4\mathrm{e}^{3y/2}}{y^3} - \frac{\mathrm{e}^{2y}}{y^3} - \frac{1}{y^2} + \frac{4\mathrm{e}^{y/2}}{y^2} - \frac{3\mathrm{e}^{y/2}}{y^2}$$

$$c_1 = -\frac{4}{y^3} + \frac{8\mathrm{e}^{y/2}}{y^3} - \frac{8\mathrm{e}^{3y/2}}{y^3} + \frac{4\mathrm{e}^{2y}}{y^3} - \frac{1}{y^2} + \frac{4\mathrm{e}^{y/2}}{y^2} - \frac{6\mathrm{e}^{y}}{y^2} + \frac{4\mathrm{e}^{3y/2}}{y^2} - \frac{\mathrm{e}^{2y}}{y^2}$$

$$c_3 = \frac{4}{y^5} - \frac{16\mathrm{e}^{y/2}}{y^5} - \frac{16\mathrm{e}^{y}}{y^5} + \frac{8\mathrm{e}^{3y/2}}{y^5} - \frac{20\mathrm{e}^{2y}}{y^5} + \frac{8\mathrm{e}^{5y/2}}{y^5} + \frac{2}{y^4} - \frac{10\mathrm{e}^{y/2}}{y^4} + \frac{16\mathrm{e}^{y}}{y^4} - \frac{12\mathrm{e}^{3y/2}}{y^4} + \frac{6\mathrm{e}^{2y}}{y^4} - \frac{2\mathrm{e}^{5y/2}}{y^4} - \frac{2\mathrm{e}^{\frac{y}{2}}}{y^3} + \frac{4\mathrm{e}^{y}}{y^3} - \frac{2\mathrm{e}^{\frac{3y}{2}}}{y^3}$$

However, one can observe that the computation of c_1, c_2, c_3 and c_4 suffers from computational inaccuracy for values of y equal to or approaching zero. Therefore, it is important to make use of their Taylor expansions

$$c_1 = 1 + y + \frac{1}{2}y^2 + \frac{1}{6}y^3 + \frac{13}{320}y^4 + \frac{7}{960}y^5 + \mathcal{O}(y^6),$$

$$c_2 = \frac{1}{2} + \frac{1}{2}y + \frac{1}{4}y^2 + \frac{247}{2880}y^3 + \frac{131}{5760}y^4 + \frac{479}{96768}y^5 + \mathcal{O}(y^6),$$

$$c_3 = \frac{1}{6} + \frac{1}{6}y + \frac{61}{720}y^2 + \frac{1}{36}y^3 + \frac{1441}{241920}y^4 + \frac{67}{120960}y^5 + \mathcal{O}(y^6),$$

$$c_4 = \frac{1}{24} + \frac{1}{32}y + \frac{7}{640}y^2 + \frac{19}{11520}y^3 - \frac{25}{64512}y^4 - \frac{311}{860160}y^5 + \mathcal{O}(y^6).$$

We commence our analysis by choosing real negative values of y and looking for a region of stability in the complex x plane where $|r| < 1$. Hence, the boundary of the stability region is determined by writing $r = \mathrm{e}^{i\theta}, \theta \in [0, 2\pi]$

The corresponding families of stability regions are plotted in the complex x plane and displayed in **Figure 1**. Note that, in this figure, the horizontal and the vertical axes represent $\mathrm{Re}(x)$ and $\mathrm{Im}(x)$, respectively. Clearly, as shown in **Figure 1**, the stability region for the ETDRK4 scheme grows larger as $y \to -\infty$. The red curve corresponds to the case $y = 0$, where the stability region of the ETDRK4 scheme coincides with that of the corresponding order fourth order Runge-Kutta (RK4) scheme.

4. Numerical Results

method for solving the fifth order KdV equation. To show the efficiency of the present method, we report the relative infinity and root mean square norm errors of the solution defined by

$$L_\infty = \frac{\max_{1jN} \left| u_j - \bar{u}_j \right|}{\max_{1jN} \left| u_j \right|}, \tag{28}$$

and

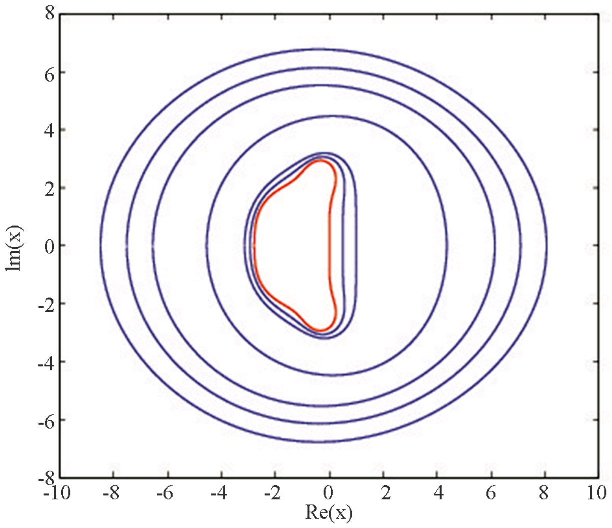

Figure 1. Stability regions in the complex x plane. The curves correspond to $y = -8; -7; -6; -4; -1; -0.5$, from the outer curve to the inner curve respectively. The inner red curve corresponds to y = 0.

$$L_2 = \sqrt{\frac{\sum_{j=1}^{N}\left(u_j - \bar{u}_j\right)^2}{\sum_{j=1}^{N}\left(\bar{u}_j\right)^2}}, \tag{29}$$

respectively, where N is the number of interior points, $\bar{u}_j$ and u_j are the exact and computed values of the solution u at point j.

In this paper, we consider two case studies depending on the set of parameters of (25) that provide multi-soliton solutions. We evaluate the performance the DSC algorithms for different time increment t, spatial discretization N, the support size of DSC kernels M and regularization parameter σ.

In our computation, the first set of parameters that we select are given by $\alpha = 5, \beta = 5, \gamma = 5$. In this case, the fifth order KdV Equation (11) is known as the Sawada-Kotera (SK) [2] equation and is given by

$$u_t + 5uu_{3x} + 5u_x u_{2x} + 5u^2 u_x + u_{5x} = 0. \tag{30}$$

The SK (30) admits multi-soliton solutions [31]. The derivation of these soliton solutions is beyond the scope of this paper. We only list them here for testing numerical procedures purposes. Single and two soliton solutions are given by

$$u(x,t) = 6\left[\ln\left(\phi(x,t)\right)\right]_{xx}, \tag{31}$$

where

$$\phi = 1 + \exp(\xi_1), \tag{32}$$

$$\phi = 1 + \exp(\xi_1) + \exp(\xi_2) + a_{12}\exp(\xi_1 + \xi_2), \tag{33}$$

respectively, with

$$\xi_i = k_i x - k_i^5 t + \delta_i \quad \text{and} \quad a_{ij} = \frac{\left(k_i - k_j\right)^2\left(k_i^2 - k_i k_j + k_j^2\right)}{\left(k_i + k_j\right)^2\left(k_i^2 + k_i k_j + k_i^2\right)} \tag{34}$$

In our computational work, we use the collocation points

$$\left\{x_1 = a, \cdots, x_i = a + (i-1)h, \cdots, x_N = b\right\}, h = \frac{|b-a|}{N-1}. \tag{35}$$

The SK equation possesses infinite conservation laws [31]. The first three conservation laws are given as follow

$$I_1 = \int_{-\infty}^{\infty} u\mathrm{d}x, I_2 = \int_{-\infty}^{\infty} u^2\mathrm{d}x, I_3 = \int_{-\infty}^{\infty}\left[\frac{1}{3}u^3 - u_x^2\right]\mathrm{d}x, \tag{36}$$

related to the mass, momentum and energy. The quantities I_1, I_2 and I_3 are applied to measure the conservation properties of the collocation scheme, calculated by

$$I_1 \approx h\sum_{j=-\infty}^{\infty} u_j, I_2 \approx h\sum_{j=-\infty}^{\infty} u_j^2, I_3 \approx h\sum_{j=-\infty}^{\infty}\left[\frac{1}{3}u_j^3 - \left(u_x\right)_j^2\right]. \tag{37}$$

The second set of parameters are chosen as $\alpha = 10, \beta = 25, \gamma = 20$. This is well-known as the Kaup-Kupershmidt (KK) [3] equation

$$u_t + 10uu_{3x} + 25u_x u_{2x} + 20u^2 u_x + u_{5x} = 0. \tag{38}$$

Multi-soliton solutions can be generated by the following nonlinear transformation of the dependent variable,

$$u(x,t) = \frac{3}{2}\left[\ln\left(\phi(x,t)\right)\right]_{xx}. \tag{39}$$

For one soliton solution, the dependent variable function is given by

$$\phi = 1 + \exp(\xi_1) + \frac{1}{16}\exp(2\xi_1), \xi_1 = k_1 x - k_1^5 t + \delta_1 \tag{40}$$

For two soliton solutions, the dependent variable function is

$$\begin{aligned} \phi = {} & 1 + \exp(\xi_1) + \exp(\xi_2) + \frac{1}{16}\exp(2\xi_1) \\ & + \frac{1}{16}\exp(2\xi_2) + a_{12}\exp(\xi_1 + \xi_2) \\ & + b_{12}\left[\exp(2\xi_1 + \xi_2) + \exp(\xi_1 + 2\xi_2)\right] \\ & + b_{12}^2\exp(2\xi_1 + 2\xi_2), \end{aligned} \tag{41}$$

with

$$a_{12} = \frac{2k_1^4 - k_1^2 k_2^2 + 2k_2^4}{2(k_1+k_2)^2 (k_1^2 + k_1 k_2 + k_2^2)},$$
$$b_{12} = \frac{(k_1-k_2)^2 (k_1^2 - k_1 k_2 + k_2^2)}{16(k_1+k_2)^2 (k_1^2 + k_1 k_2 + k_2^2)}. \quad (42)$$

The KK equation possesses infinite conservation laws [31], the first three are given as follows

$$I_1 = \int_a^b u\mathrm{d}x, I_2 = \int_a^b u^2 \mathrm{d}x, I_3 = \int_a^b \left[\frac{1}{3}u^3 - \frac{1}{8}u_x^2\right]\mathrm{d}x. \quad (43)$$

The quantities I_1, I_2 and I_3 are applied to measure the conservation properties of the collocation scheme, calculated by

$$I_1 \approx h\sum_{j=-\infty}^{\infty} u_j, I_2 \approx h\sum_{j=-\infty}^{\infty} u_j^2, I_3 \approx h\sum_{j=-\infty}^{\infty}\left[\frac{1}{3}u_j^3 - \frac{1}{8}(u_x)_j^2\right] \quad (44)$$

In next sections, we study the propagation and the interaction of single and two soliton solutions, respectively.

4.1. Propagation of Single Solitons

In our numerical experiments, we first model the motion of a single soliton of the SK (30) and KK (38) equations. For the SK equation, the initial condition is taken from the exact solutions (32) and (31) at initial profile. Whereas for the KK equation, the initial condition is taken from the exact solutions (40) and (39) at initial profile. The boundary conditions in both cases are chosen so that

$$u(-\infty, t) = 0 \text{ and } u(\infty, t) = 0. \quad (45)$$

In the first computation, we would like to investigate the convergence of the DSC method with respect to the number of grid points N and the DSC bandwidth M. The values of the parameters used in our numerical experiments are: $k_1 = 0.4, \delta_1 = 0$ and $\delta t = 0.001$ in both cases of the SK and KK equations. In each case, the soliton moves to the right across the space interval $x \in [-100, 100]$ when the time interval is $t \in [0, 1500]$. The choice of the DSC bandwidth M and the regularizer parameter σ is done according to the conditions (10). Hence if $M = 16$ then $\sigma \approx 2.5h$. If $M = 32$ then $\sigma \approx 3.2h$. If $M = 64$ then $\sigma \approx 6.2h$.

Figure 2 illustrates the convergence of the DSC with respect to the number of the grid points N and the DSC bandwidth M. We observe that numerical soliton solutions of the DSC method converge towards the exact soliton solutions as the number of grid points N increases. We remark that the convergence of the DSC method also relies on the bandwidth M. The results in **Figure 2** shows that the case $M = 64$ gives a better convergence, the case $M = 16$ gives the worst convergence, whereas when $M = 32$ we have an intermediate convergence.

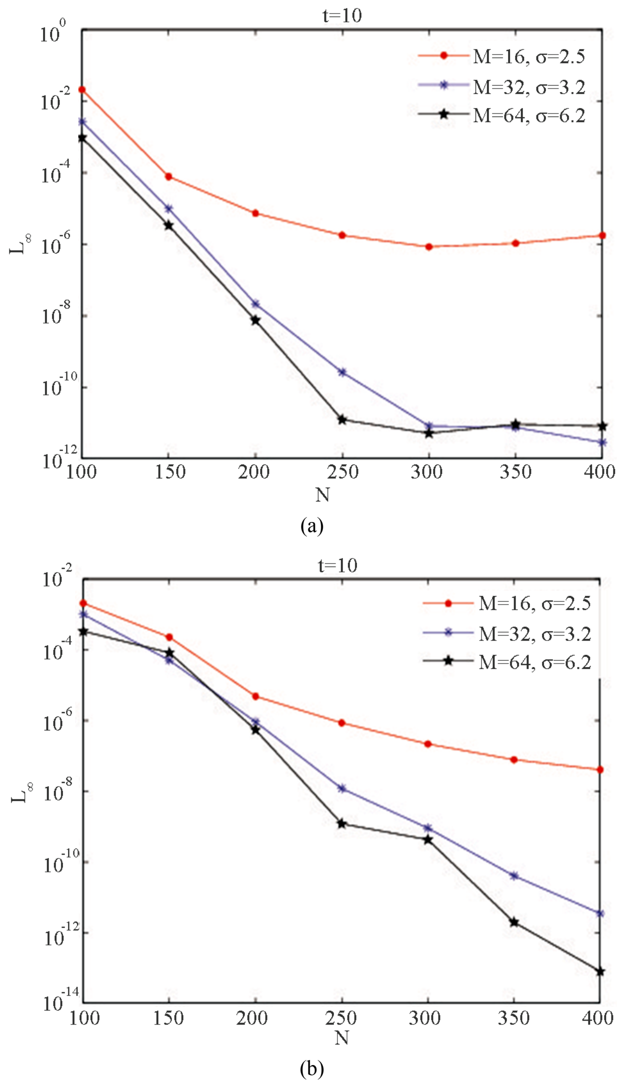

Figure 2. Convergence the DSC method for the propagation of single soliton solution of the SK (a) and the KK (b) equations at $t = 10$ with $k_1 = 0.4$, $\delta_1 = 0$ and $\delta t = 0.001$ and $x \in [-100, 100]$.

In fact when the bandwidth M is large, the DSC method behaves like a global and detains exponential accuracy, whereas for a small value of M, the DSC behaves like a local method such as finite difference methods. This result is stated by Theorem 2.1.

Figure 3 represents numerical propagation of one soliton solutions of the SK (a) and the KK (b) equations. These propagations occur for a long period of time with no spurious oscillations.

In the next experiment, we compute the error norms L_∞, L_2 and conservation quantities I_1, I_2 and I_3. The results are shown in **Table 1** for one soliton solution of the SK equation and in **Table 2** for one soliton solution of the KK equation.

From the numerical results given in **Tables 1** and **2** it

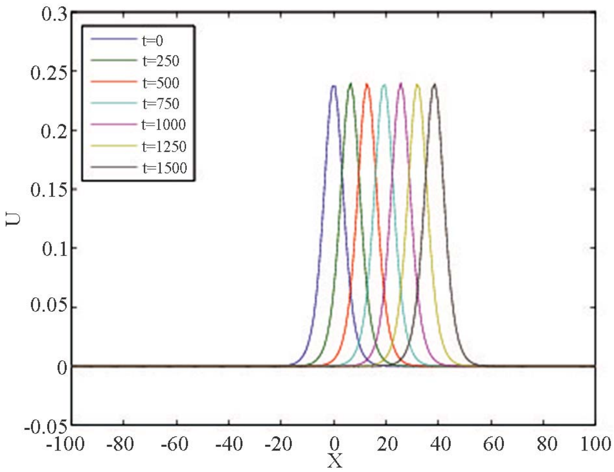

(a)

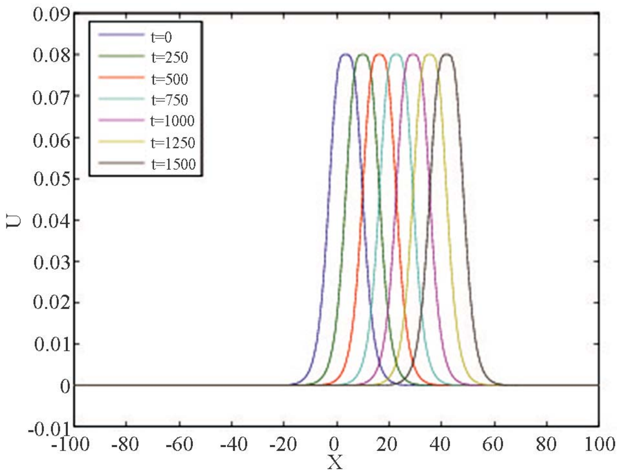

(b)

Figure 3. Propagation of single soliton solution of the SK (a) and the KK (b) equations with $k_1 = 0.4$, $\delta_1 = 0$, $\delta t = 0.001$, $N = 200$ and $x \in [-100,100]$.

is observed that throughout the simulation, the error norms L_∞ and L_2 are of magnitude 10^{-4} at a long period of time $t = 1500$. Whereas the invariants I_1, I_2 and I_3 at a given time t are equal to those of the initial value. Our scheme conserve, the mass, momentum and energy.

4.2. Interaction of Two Solitons

This computational work is related to the interaction of two soliton solutions of SK (30) and KK (38) equations having different amplitudes and travelling in the same direction. For the SK equation, the initial condition is taken from the exact solutions (33) and (31) at initial profile; whereas for the KK equation, the initial condition is taken from the exact solutions (41) and (39) at initial profile. The boundary conditions in both cases are chosen so that

Table 1. Invariants and errors for a single soliton of the SK equation. $k_1 = 0.4$, $\delta_1 = 0$, $N = 200$, $\delta t = 0.1$ and $x \in [-100,100]$.

t	L_∞	L_2	I_1	I_2	I_3
50	0	0	2.4000	0.3840	0.0123
250	2.9354E-7	6.4931E-7	2.4000	0.3840	0.0123
500	4.5926E-7	1.2687E-6	2.4000	0.3840	0.0123
750	1.1870E-6	2.6083E-6	2.4000	0.3840	0.0123
1000	7.2493E-6	1.6938E-5	2.4000	0.3840	0.0123
1250	3.8777E-5	9.0258E-5	2.4000	0.3840	0.0123
1500	3.0826E-4	7.1035E-4	2.4000	0.3840	0.0123

Table 2. Invariants and errors for a single soliton of the KK equation. $k_1 = 0.4$, $\delta_1 = 0$, $N = 200$, $\delta t = 0.1$ and $x \in [-100,100]$.

t	L_∞	L_2	I_1	I_2	I_3
50	0	0	1.2000	0.0730	0.0015
250	2.4116E-7	5.0563E-7	1.2000	0.0730	0.0015
500	4.3930E-7	9.6785E-7	1.2000	0.0730	0.0015
750	6.4347E-7	1.4086E-6	1.2000	0.0730	0.0015
1000	7.2969E-7	1.8528E-6	1.2000	0.0730	0.0015
1250	1.1567E-6	2.3038E-6	1.2000	0.0730	0.0015
1500	1.2106E-6	2.7218E-6	1.2000	0.0730	0.0015

$$u(-\infty,t) = 0 \text{ and } u(\infty,t) = 0. \quad (46)$$

To allow the interaction to occur, the experiment was run from $t = 0$ to 400 in the region $[-100,100]$. **Figure 4** shows the interaction of two soliton solutions of the SK (top) and KK (bottom) equations for $k_1 = 0.4$, $k_2 = 0.6$, $\phi_1 = 0$, $\phi_2 = 30$, $N = 200$, $\delta t = 0.001$ and $x \in [-100,100]$. It can be seen that the faster pulse interacts with and emerges ahead of the lower pulse with the shape and velocity of each soliton retained.

We also investigate the convergence of the DSC method with respect to the number of the grid points N and the DSC bandwidth M as we did in the case of one soliton solutions.

All the results are shown in **Figure 5**. We observe that numerical soliton solutions obtained by means of the DSC method converge to the exact soliton solutions as the number of grid points N increases. We also observe that the convergence of the DSC method relies on the bandwidth M. The results on **Figure 5** show that the case $M = 64$ gives a better convergence, the case $M = 16$ gives the worst convergence, whereas when

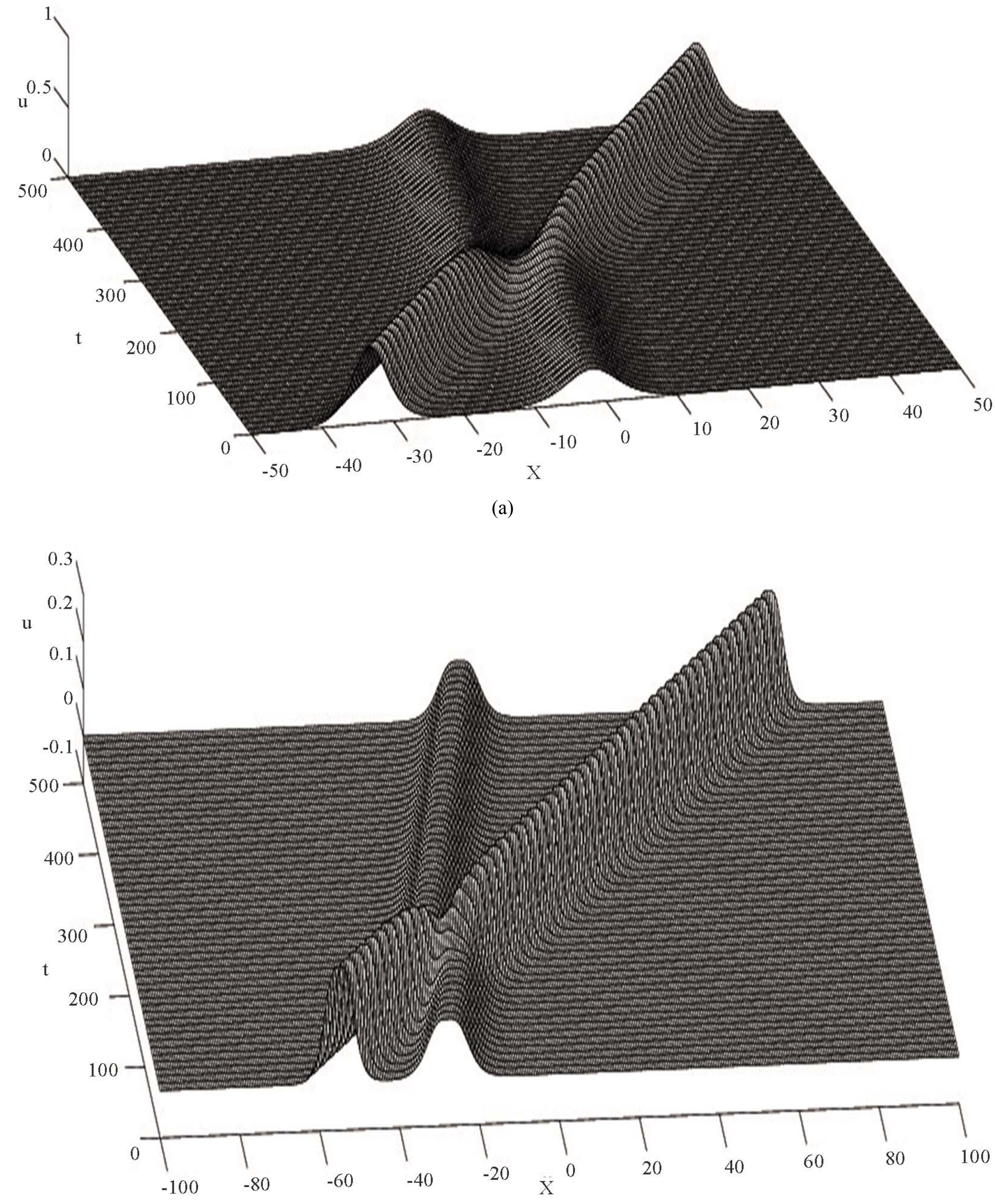

(a)

(b)

Figure 4. Interaction of two soliton solutions of the SK (top) and the KK (bottom) equations with $k_1 = 0.4$, $k_2 = 0.6$, $\phi_1 = 0$, $\phi_2 = 30$, $N = 200$, $\delta t = 0.001$ and $x \in [-100, 100]$.

$M = 32$ we have an intermediate convergence. In fact when the bandwidth M is large, the DSC method behaves like a global and detains exponential accuracy, whereas for a small value of M, the DSC behaves like a local method such as finite difference methods.

In addition, we compute the error norms L_∞, L_2 and conservation quantities I_1, I_2 and I_2 are computed. The result are shown in **Table 3** for two soliton solutions of the SK equation and in **Table 4** for two soliton solutions of the KK equation.

From the numerical results given in **Table 3** it is observed that throughout the simulation, the error norms L_∞ and L_2 are of magnitude 10^{-5} at a long period of time 400, whereas the error norms L_∞ and L_2 (**Table 4**) are of magnitude 10^{-8} at a long period of time. The invariants I_1, I_2 and I_2 at a given time t are equal to those of the initial value. Numerical checks on the conservation mass, momentum and energy show that the

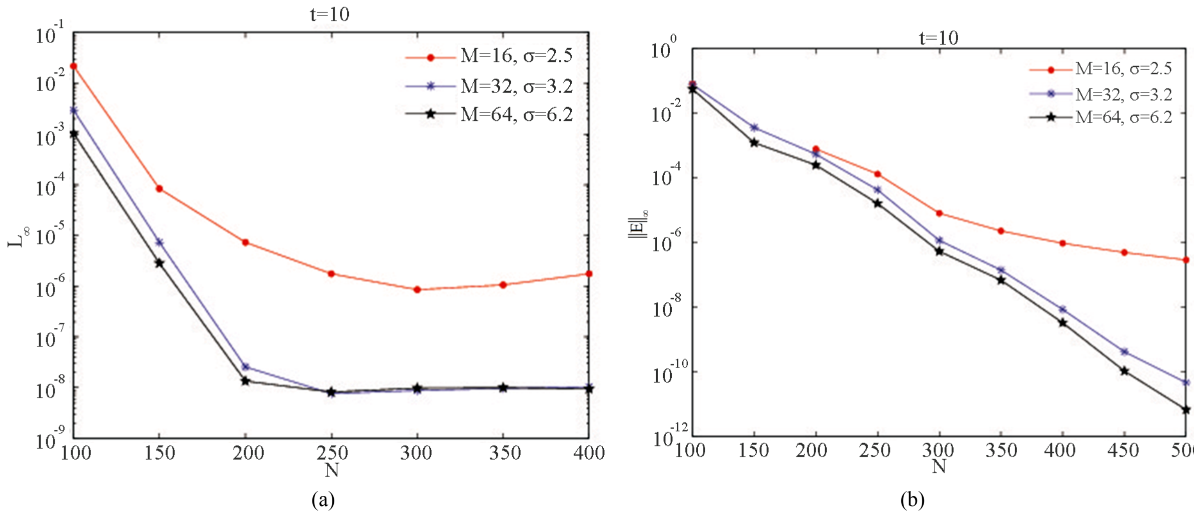

Figure 5. Convergence the DSC method for the interaction of two soliton solutions of the SK (a) and the KK (b) equations with $k_1 = 0.4$, $k_2 = 0.6$, $\phi_1 = 0$, $\phi_2 = 30$, $\delta t = 0.001$ and $x \in [-100, 100]$.

Table 3. Invariants and errors for interaction of two solitons of the SK equation. $k_1 = 0.4$, $k_2 = 0.6$, $\phi_1 = 0$, $\phi_2 = 30$, $\delta t = 0.001$, $N = 200$, $x \in [-100, 100]$.

t	L_∞	L_2	I_1	I_2	I_3
50	0	0	6.0000	1.6799	0.1056
100	2.3576e-008	4.6137e-008	6.0000	1.6736	0.1056
200	2.6207e-007	6.5108e-007	6.0000	1.5118	0.1056
300	7.2470e-007	2.2323e-006	6.0000	1.6552	0.1056
400	7.7486e-005	2.3119e-004	6.0000	1.6796	0.1056

Table 4. Invariants and errors for interaction of two solitons of the KK equation. $k_1 = 0.4$, $k_2 = 0.6$, $\phi_1 = 0$, $\phi_2 = 30$, $\delta t = 0.001$, $N = 450$, $x \in [-100, 100]$.

t	L_∞	L_2	I_1	I_2	I_3
50	0	0	3.0000	0.3194	0.0132
100	4.6168e-009	5.2241e-009	3.0000	0.3194	0.0132
200	2.6397e-009	3.5804e-009	3.0000	0.3194	0.0132
300	2.6443e-009	4.1965e-009	3.0000	0.3194	0.0132
400	8.4855e-009	1.2871e-008	3.0000	0.3194	0.0123

three quantities remain constant with respect to time.

5. Conclusion

We studied the application of the combined DSC scheme in space discretization and the ETDRK4 for time discretization to solve the SK and KK equations. We considered the case of the propagation of a single soliton and the interaction of two solitons. Numerical results showed that the DSC method converges exponentially with respect to the number of grid points N and the bandwidth M. Numerical checks on the conservation mass, momentum and energy revealed that the three quantities remain constant with respect to time t. The DSC scheme is a robust and reliable numerical method of the fifth order KdV equation. We are currently investigating the utility of the DSC method to solve the GRLW equation.

6. Acknowledgements

E. Pindza acknowledges the financial support from Brad Welch through RidgeCape.

REFERENCES

[1] P. D. Lax, "Integrals of Nonlinear Equations of Evolution and Solitary Waves," *Communications on Pure and Applied Mathematics*, Vol. 21, No. 5, 1968, pp. 467-490. http://dx.doi.org/10.1002/cpa.3160210503

[2] K. Sawada and T. Kotera, "A Method for Finding N-Soliton Solutions for the KdV Equation and KdV-Like Equations," *Progress of Theoretical Physics*, Vol. 51, No. 5, 1974, pp. 1355-1367. http://dx.doi.org/10.1143/PTP.51.1355

[3] A. P. Fordy and J. Gibons, "Some Remarkable Nonlinear Transformations," *Physics Letters*, Vol. *A*75, No. 5, 1980, p. 325. http://dx.doi.org/10.1016/0375-9601(80)90829-4

[4] M. Ito, "An Extension of Nonlinear Evolution Equations of the KdV (mKdV) Type to Higher Orders," *Journal of the Physical Society of Japan*, Vol. 49, 1980, pp. 771-778. http://dx.doi.org/10.1143/JPSJ.49.771

[5] J. Shen, "A New Dual-Petrov-Galerkin Method for Third and Higher Odd-Order Differential Equations: Application to the KdV Equation," *SIAM Journal on Numerical*

Analysis, Vol. 41, No. 5, 2003, pp. 1595-1619. http://dx.doi.org/10.1137/S0036142902410271

[6] J. Shen and L. L. Wang, "Laguerre and Composite Legendre-Laguerre Dual-Petrov-Galerkin Methods for Third-Order Equations," *DCDS-B*, Vol. 6, No. 6, 2006, pp. 1381-1402. http://dx.doi.org/10.3934/dcdsb.2006.6.1381

[7] J. M. Yuan, J. Shen and J. Wu, "A dual-Petrov-Galerkin Method for the Kawahara-Type Equation," *Journal of Scientific Computing*, Vol. 34, No. 1, 2008, pp. 48-63. http://dx.doi.org/10.1007/s10915-007-9158-4

[8] G. W. Wei, "Discrete Singular Convolution for the Fokker-Planck Equation," *Journal of Chemical Physics*, Vol. 110, 1999, pp. 8930-8942. http://dx.doi.org/10.1063/1.478812

[9] W. Bao, F. Sun and G. W. Wei, "Numerical Methods for the Generalized Zakharov System," *Journal of Computational Physics*, Vol. 190, No. 1, 2003, pp. 201-228. http://dx.doi.org/10.1016/S0021-9991(03)00271-7

[10] G. W. Wei, Y. B. Zhao and Y. Xiang, "Discrete Singular Convolution and Its Application to the Analysis of Plates with Internal Supports. Part 1: Theory and Algorithm," *International Journal Numerical Methods in Engineering*, Vol. 55, No. 8, 2002, pp. 913-946. http://dx.doi.org/10.1002/nme.526

[11] G. W. Wei, "Vibration Analysis by Discrete Singular Convolution," *Journal of Sound Vibration*, Vol. 244, No. 3, 2001, pp. 535-553. http://dx.doi.org/10.1006/jsvi.2000.3507

[12] G. W. Wei, "A New Algorithm for Solving Some Mechanical Problems," *Computational Methods in Applied Mechanical Engineering*, Vol. 190, No. 15, 2001, pp. 2017-2030. http://dx.doi.org/10.1016/S0045-7825(00)00219-X

[13] Y. C. Zhou and G. W. Wei, "High-Resolution Conjugate Filters for the Simulation of Flows," *Journal of Computational Physics*, Vol. 189, No. 1, 2003, pp. 150-179.

[14] G. Bao, G. W. Wei and S. Zhao, "Numerical Solution of the Helmholtz Equation with High Wave Numbers," *International Journal of Numerical Methods in Engineering*, Vol. 59, No. 3, 2004, pp. 389-408. http://dx.doi.org/10.1002/nme.883

[15] G. Bao, G. W. Wei and S. Zhao, "Local Spectral Time-Domain Method for Electromagnetic Wave Propagation," *Optic Letters*, Vol. 28, No. 7, 2003, pp. 513-515. http://dx.doi.org/10.1364/OL.28.000513

[16] Z. J. Hou and G. W. Wei, "A New Approach for Edge Detection," *Pattern Recognition*, Vol. 35, No. 7, 2002, pp. 1559-1570. http://dx.doi.org/10.1016/S0031-3203(01)00147-9

[17] E. Pindza and E. Maré, "Discrete Singular Convolution and Exponential Time Integrators for Solving the Generalized Korteweg-de Vries Equation," Technical Report UPWT 2013/14, University of Pretoria, Pretoria.

[18] S. Y. Yang, Y. C. Zhou and G. W. Wei, "Comparison of the Discrete Singular Convolution Algorithm and the Fourier Pseudospectral Methods for Solving Partial Differential Equations," *Computer Physics Communications*, Vol. 143, No. 2, 2002, pp. 113-135. http://dx.doi.org/10.1016/S0010-4655(01)00427-1

[19] G. W. Wei, Y. B. Zhao and Y. Xiang, "A Novel Approach for the Analysis of High Frequency Vibrations," *Journal of Sound and Vibration*, Vol. 257, No. 2, 2002, pp. 207-246. http://dx.doi.org/10.1006/jsvi.2002.5055

[20] A. K. Kassam and L. N. Trefethen, "Fourth-Order Time Stepping for Stiff PDEs," *SIAM Journal of Scientific Computing*, Vol. 26, No. 4, 2005, pp. 1214-1233. http://dx.doi.org/10.1137/S1064827502410633

[21] L. N. Trefethen and H. M. Gutknecht, "The Carathéodory-Fejér Method for Real Rational Approximation," *SIAM Journal on Numerical Analysis*, Vol. 20, No. 2, 1983, pp. 420-436. http://dx.doi.org/10.1137/0720030

[22] G. W. Wei, "Discrete Singular Convolution for the Sine-Gordon Equation," *Physica D*, Vol. 137, No. 3, 2000, pp. 247-259. http://dx.doi.org/10.1016/S0167-2789(99)00186-4

[23] L. W. Qian, "On the Regularized Whittaker-Kotel'nikov-Shannon Sampling Formula," *Proceedings of American Mathematical Society*, Vol. 131, No. 4, 2003, pp. 1169-1176. http://dx.doi.org/10.1090/S0002-9939-02-06887-9

[24] R. X. Yao, C. Z. Qu and Z. B. Li, "On Properties of New Parameterized 5th-Order Nonlinear Evolution Equation," *Chaos, Solitons and Fractals*, Vol. 21, No. 5, 2004, pp. 1145-1152. http://dx.doi.org/10.1016/j.chaos.2003.12.078

[25] E. Pindza, "Spectral Difference Methods for Solving Equation of the KdV Hierarchy," MSc Thesis, University of Stellenbosch, Stellenbosch, 2008.

[26] B. Minchev and W. Wright, "A Review of Exponential Integrators for First Order Semi-Linear Problems," Technical Report 2, The Norwegian University of Science and Technology, 2005.

[27] S. M. Cox and P. C. Matthews, "Exponential Time Differencing for Stiff Systems," *Journal of Computational Physics*, Vol. 176, No. 2, 2002, pp. 430-455. http://dx.doi.org/10.1006/jcph.2002.6995

[28] Y. Saad, "Analysis of Some Krylov Subspace Approximations to the Matrix Exponential Operator," *SIAM Journal of Numerical Analysis*, Vol. 29, No. 1, 1992, pp. 209-228. http://dx.doi.org/10.1137/0729014

[29] M. Hochbruck and C. Lubich, "On Krylov Subspace Approximations to the Matrix Exponential Operator," *SIAM Journal of Numerical Analysis*, Vol. 34, No. 5, 1997, pp. 1911-1925. http://dx.doi.org/10.1137/S0036142995280572

[30] T. Schmelzer and L. N. Trefethen, "Evaluating Matrix Functions for Exponential Integrators via Carathéodory-Fejér Approximation and Contour Integrals," *Electronic Transactions on Numerical Analysis*, Vol. 29, 2007, pp. 1-18.

[31] A. Nuseir, "Symbolic Computation of Exact Solutions of Nonlinear Partial Differential Equations Using Direct Methods," PhD Thesis, Colorado School of Mines, 1997.